Electronic Supporting Information

Active Tumor-Targeting Luminescent Gold Clusters with Efficient Urinary Excretion

Xiaojuan Wang, Hua He, Yanan Wang, Junying Wang, Xing Sun, Hai Xu, Werner M. Nau,* Xiaodong Zhang* and Fang Huang*

1. Experimental Section

Hydrogen tetrachloroaurate ($HAuCl_4 \bullet 4H_2O$) was from Shanghai Jiuyue Chemical Company. The CRGDS peptide was synthesized and purified by ChinaPeptides Co., Ltd. (Shanghai, China). All chemicals involved in this work were used without any further purification. Aqueous solutions were freshly prepared with ultrapure water(≥18.2MΩ), purified on a Millipore system (Millipore, USA). For the nanocluster synthesis, aqueous solutions of HAuCl4 (20 mM) and CRGDS (100 mM) were prepared separately in the dark. Then, 0.4 ml of the CRGDS solution and 1.00 ml of the HAuCl4 solution were mixed with 8.60 ml of water at 25 °C and the reaction mixture was heated to 80 °C for 17 h. The obtained aqueous solutions of AuNCs were ultra-filtered three times (6000 rpm, 10 min) with PBS to remove excess reagents using Amicon Ultra Centrifugal Filter Units (10kDa cut-off, Millipore).

Animal welfare and animal experiments were carried out in accordance with the Guide for the Care and Use of Laboratory Animals (Ministry of Science and Technology of China, 2006), and were approved by the animal ethics committee of the Institute of Radiation Medicine, Chinese Academy of Medical Sciences (CAMS).

Spectroscopy. Ultraviolet-visible (UV-Vis) spectra were recorded on a Shimadzu UV-2450 spectrophotometer. Fluorescence spectra were collected on a Hitachi F-2500 fluorometer. High-resolution transmission electron microscopic (HRTEM) images were measured on a JEM-2100 electron microscope at 200 kV. The size distributions of the synthesized AuNCs were determined by DLS on a NanoZS Zetasizer (Malvern, UK).

Confocal fluorescence imaging. U87 (human primary glioblastoma), A549 (human non-small lung carcinoma), HeLa (human cervical cancer), HepG-2 (human hepatocellular carcinoma), and MCF-7 (human breast adenocarcinoma) cells were used to verify the active-targeting cell internalization of

CRGDS–AuNCs. The cells (1×10^5) were seeded onto 12-mm sterile coverslips in a 24-well plate and cultured for 24 h, washed thrice with PBS, and then incubated with CRGDS–AuNCs (300 μg/mL) at 37 ºC for 5 h. After washing thrice with cold PBS, the cells were fixed for 20 min in 200 μL of 4% paraformaldehyde. After fixation, the cells were washed thrice with PBS. The side of the coverslip with the fixed cells was topped by a glass slide with 5 μL of 50% glycerol/PBS (v/v). Fluorescence images were taken with a confocal laser scanning microscope (CLSM, Nikon Al, Nikon, Japan). CRGDS–AuNCs were excited at 405 nm, and their emission was collected between 570-617 nm.

Cell viability assay. HeLa and MCF-7 cells were seeded on 96-well plates at 2×10^4 cells/well in 100 μL of DMEM medium supplemented with 10% FBS. The plates were incubated for 24 h at 37 °C in a humidified 5% CO_2 atmosphere. On the day of the experiments, the cells were washed with PBS buffer and incubated with fresh medium-containing CRGDS–AuNCs at 37 °C for 12 or 24 h. As a control, only complete medium was added. The cells were then washed twice with PBS, and 20 μL of MTT solution (5 mg/mL) was added subsequently to each well. The plates were incubated at 37 °C for 4 h. The precipitated formazan was dissolved in 150 μL of dimethyl sulfoxide. The absorbance of each sample at 490 nm was measured by using a microplate autoreader (Molecular Devices, M2e). The cell viability ratio was calculated according to $A_{490\ nm}/A_{0,490\ nm}$ (control).

***In vivo* imaging.** Male nude mice were used as tumor-bearing models and C57 male mice were used for the urinary excretion tests. All animals acclimated to the animal facility for at least 48 h before experimentation. For surgery, mice were anesthetized with chloral hydrate. The tumor-bearing models were generated by subcutaneous injection of 2×10^6 tumor cells suspended in 50 μL of PBS into the right shoulder of the male nude mice. The tumor was allowed to grow about 7 days after inoculation to reach 100–120 mm^3 for the imaging and biodistribution studies. 200 μL of CRGDS–AuNCs at a concentration of 8 mg/ml were injected into the tail vein of the male nude mice after

anesthetization (three mice per group). The tumor-bearing nude mouse was then imaged by using an *in vivo* fluorescence imaging system (Caliper Inc.). Visible light with a central wavelength of 532 nm was used as the excitation source. The signal collection range was 550–800 nm with an exposure time of 126 ms. Autofluorescence was removed by using the spectral unmixing software.

Animal biodistribution studies. Tumor-bearing male nude mice, which had been injected with CRGDS–AuNCs, were re-anesthetized before euthanizing them by cervical dislocation at 24 h p.i.. Organs of interest, including heart, liver, spleen, lung, kidney, bladder, tumor, and testis, were collected and analyzed by *ex vivo* fluorescence imaging. The photoluminescence intensity of the samples was measured at an excitation wavelength of 532 nm.

Image processing and analysis. The fluorescence microscopic images were processed with Nikon's NIS-Elements AR software on the CLSM instrument. Briefly, for each individual image the average fluorescence intensities of the cell-occupying area was calculated and corrected for the fluorescence intensity of the blank area in the same image to obtain comparable fluorescence intensity. For the *in vivo* experiments, the average fluorescence intensities of the tumor area in each image were calculated and profiled directly. For the *ex vivo* experiment, the average fluorescence intensities of organ images from non-injected mice were calculated and subtracted from the average fluorescence intensities of the same organ from AuNCs-injected mice to afford corrected fluorescence intensity .

Urinary excretion studies. 200 μL of CRGDS–AuNCs at a concentration of 8 mg/ml were injected through the tail vein of C57 mice. Mice were housed in special cages to allow for the collection of urine at different p.i. time points. The luminescence of the urine was measured with a Hitachi F-4600 fluorescence spectrophotometer and subtracted with the autofluorescence of the pure urine to calculate the CRGDS–AuNCs content.

2. Supporting Text: Additional Background on AuNCs Previously Applied for Fluorescence Tumor Detection

AuNCs that are synthesized using bovine serum albumin (BSA) and the tripeptide glutathione (GSH) as ligands have been previously applied as passive-targeting agents for *in vivo* tumor diagnosis and therapy.[1-6] Both of them accumulated selectively in the tumor by the EPR effect and produced fluorescence signals. *In vivo* toxicity investigations indicated that compared with GSH–AuNCs, BSA–AuNCs show a less efficient renal clearance and higher *in vivo* toxicity, mainly due to their relatively large hydrodynamic diameter (HD).[5] Since the gold cluster cores of GSH–AuNCs and BSA–AuNCs have similar size, it is therefore reasonable to deduce that the difference between the two types of ligands, short peptides *versus* proteins, leads to the varied HDs and, in turn, the distinct *in vivo* toxicity. Thus, it appeared desirable to choose small molecules, such as short peptides, as protecting ligands to synthesize AuNCs for *in vivo* application.

Although the GSH peptide serves as an excellent protecting agent, it does not possess any tumor-recognizing capability. In order to obtain the tumor specificity, a folic acid-modified polymeric system has been applied to conjugate with GSH–AuNCs.[7,8] Although the resulting system was capable of active targeting and imaging of the cancer cells, the size of the system was again dramatically increased, with the known adverse effects. Active-targeting AuNCs were also achieved by conjugating folic acid directly to protein-protected AuNCs (BSA–AuNCs and ovalbumin–AuCNs).[9-11] But taking account the large HD of BSA–AuNCs and the additional conjugated layers, these functional agents do not address the low efficiency of renal clearance of the unmodified BSA–AuNCs. Consequently, active-targeting gold clusters with stable fluorescence, good tumor-targeting capability, and excellent excretion profiles have not become available.

3. Supporting Figures

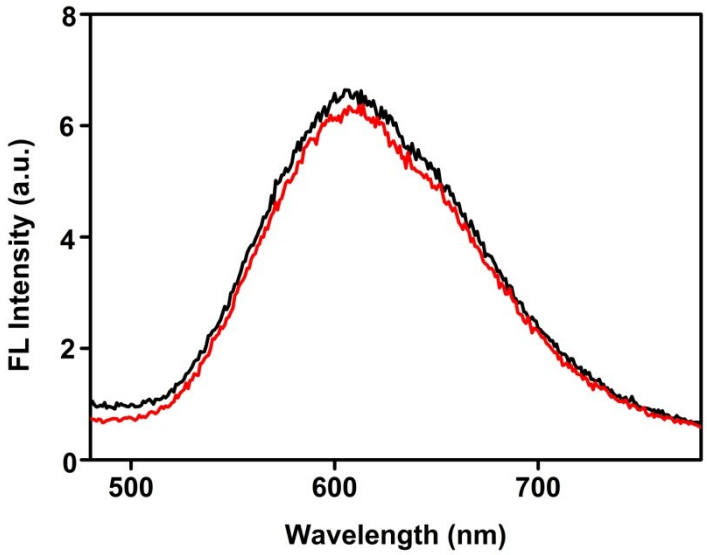

Figure S1. Fluorescence emission spectra of freshly synthesized CRGDS–AuNCs colloids (black) and after storage at –4 °C for 3 months (red), λ_{ex} = 400 nm.

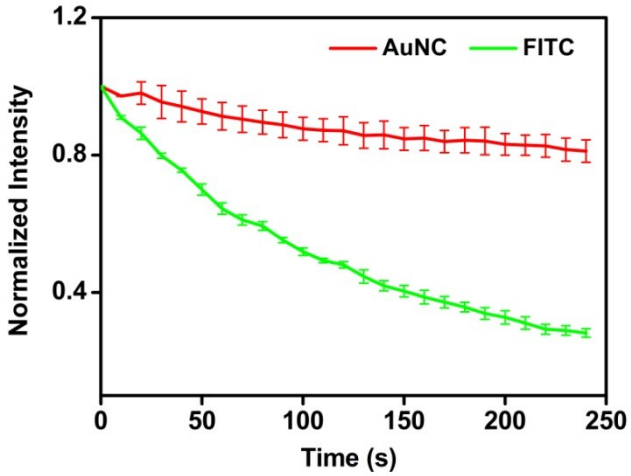

Figure S2. Fluorescence intensity depletion profiles of CRGDS–AuNCs and FITC under laser irradiation.

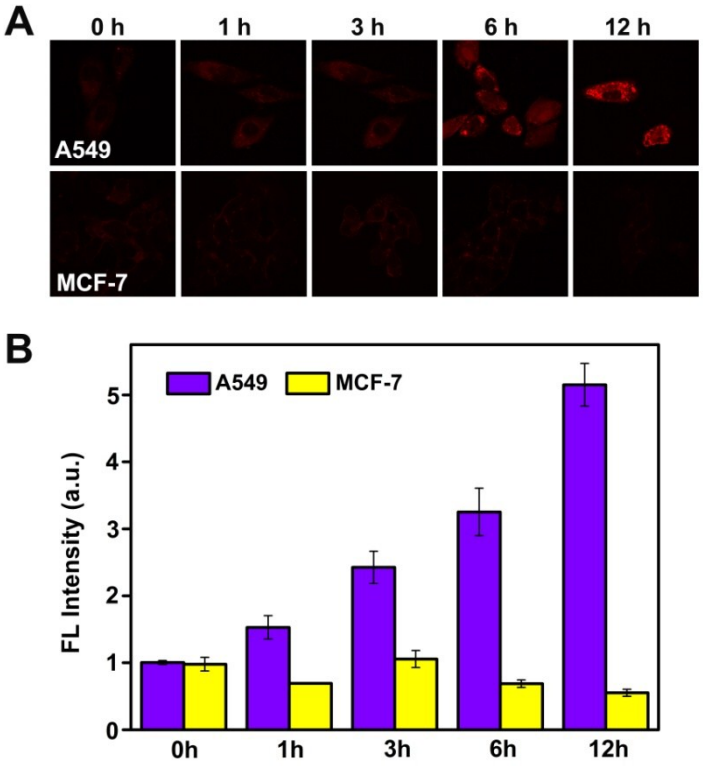

Figure S3. Specific labelling of targeting cells with CRGDS–AuNCs. (a) Confocal laser scanning microscopy of A549 and MCF-7 cells after incubation with CRGDS–AuNCs (300 μg/mL) at 37 °C for 0, 1, 3, 6, and 12 h. (b) Time-dependent cellular uptake of CRGDS–AuNCs; data are displayed as means ± standard deviation with $n = 3$.

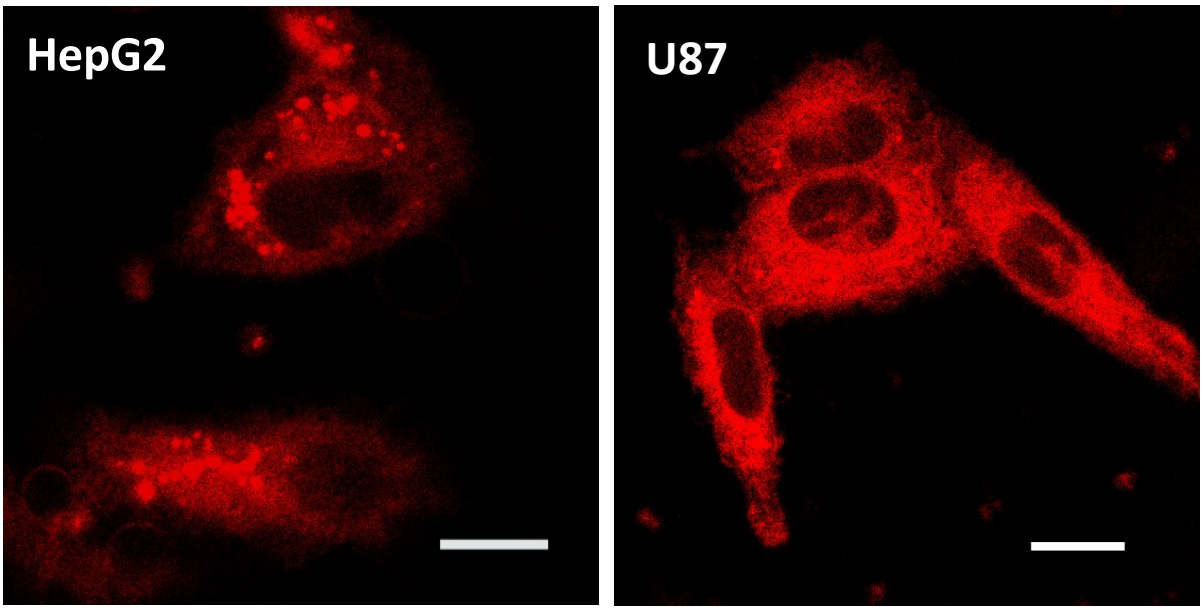

Figure S4. Magnification images of HepG2 and U87 cells after incubation with CRGDS-AuNCs containing medium for 5 h (scale bar is 20 μm).

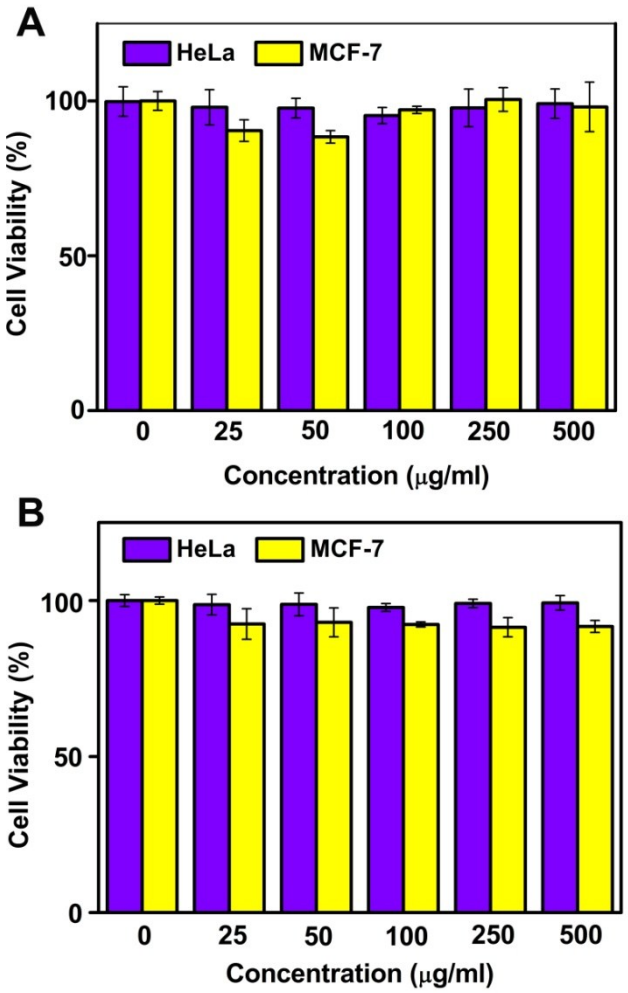

Figure S5. MTT assays illustrating the percentage viability of HeLa and MCF-7 cells upon exposure to different concentrations of CRGDS–AuNCs for (A) 12 h and (B) 24 h. The data are displayed as means ± standard deviation with $n = 6$.

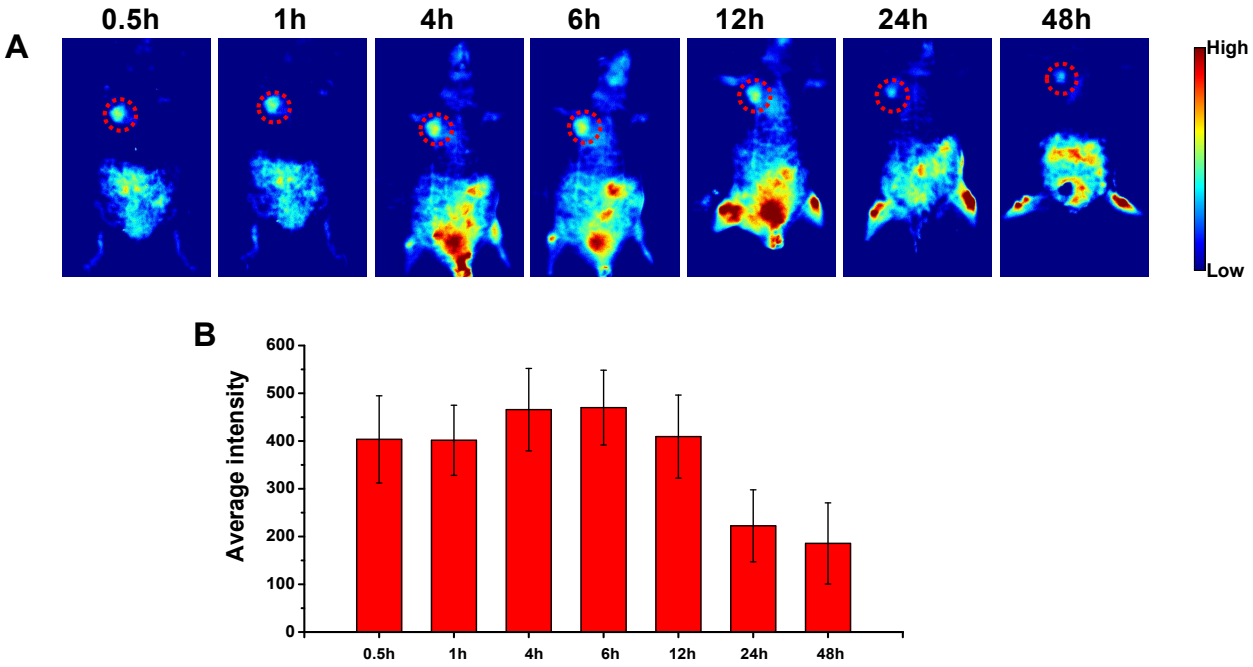

Figure S6. .(A) *In vivo* fluorescence imaging of U87 tumor-bearing nude mice after intravenous injection of CRGDS–AuNCs. Red circles indicate the tumor sites. (B) Quantification of fluorescence intensity of tumor sites. The data are displayed as means ± standard deviation with $n = 3$.

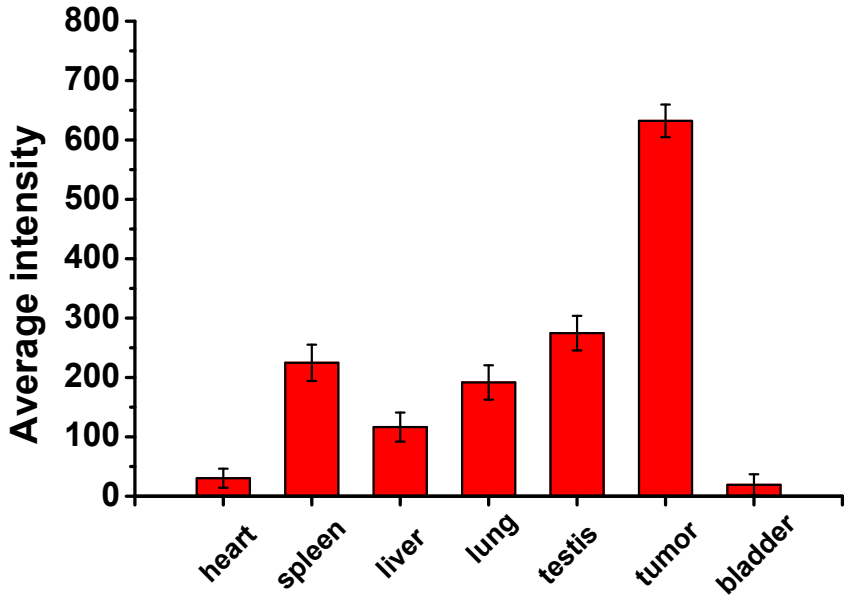

Figure S7. Bio-distribution of intravenously injected CRGDS–AuNCs based on the quantification of *ex vivo* fluorescence imaging of organs and tumors removed 48 h p.i. from U87 tumor-bearing mice.

References

1. X. Wu, X. He, K. Wang, C. Xie, B. Zhou and Z. Qing, *Nanoscale*, 2010, **2**, 2244-2249.
2. J. Liu, M. Yu, C. Zhou, S. Yang, X. Ning and J. Zheng, *J. Am. Chem. Soc.*, 2013, **135**, 4978-4981.
3. C. Zhou, M. Long, Y. Qin, X. Sun and J. Zheng, *Angew. Chem. Int. Ed.*, 2011, **50**, 3168-3172.
4. C. Zhou, G. Hao, P. Thomas, J. Liu, M. Yu, S. Sun, O. K. Öz, X. Sun and J. Zheng, *Angew. Chem. Int. Ed.*, 2012, **51**, 10118-10122.
5. X.-D. Zhang, Z. Luo, J. Chen, X. Shen, S. Song, Y. Sun, S. Fan, F. Fan, D. T. Leong and J. Xie, *Adv. Mater.*, 2014, **26**, 4565-4568.
6. P. Huang, J. Lin, S. Wang, Z. Zhou, Z. Li, Z. Wang, C. Zhang, X. Yue, G. Niu, M. Yang, D. Cui and X. Chen, *Biomaterials*, 2013, **34**, 4643-4654.
7. D. Chen, Z. Luo, N. Li, J. Y. Lee, J. Xie and J. Lu, *Adv. Funct. Mater.*, 2013, **23**, 4324-4331.
8. C. Zhang, C. Li, Y. Liu, J. Zhang, C. Bao, S. Liang, Q. Wang, Y. Yang, H. Fu, K. Wang and D. Cui, *Adv. Funct. Mater.*, 2015, **25**, 1314-1325.
9. A. Retnakumari, S. Setua, D. Menon, P. Ravindran, H. Muhammed, T. Pradeep, S. Nair and M. Koyakutty, *Nanotechnology*, 2010, **21**, 055103.
10. J. Qiao, X. Mu, L. Qi, J. Deng and L. Mao, *Chem. Commun.*, 2013, **49**, 8030-8032.
11. H. Chen, S. Li, B. Li, X. Ren, S. Li, D. M. Mahounga, S. Cui, Y. Gu and S. Achilefu, *Nanoscale*, 2012, **4**, 6050-6064.